Thin Solid Films 699 (2020) 137907

Contents lists available at ScienceDirect

Thin Solid Films

journal homepage: www.elsevier.com/locate/tsf

Decoration of suspended single-walled carbon nanotubes with soft-landed size-selected metal nanoparticles

Malak Khojasteh[a,b], Matthew H. Mecklenburg[c], Patrick J. Edwards[a], Jacques Lefebvre[d], Jianfu Ding[d], Patrick R.L. Malenfant[d], Vitaly V. Kresin[a,*]

[a] Department of Physics and Astronomy, University of Southern California, Los Angeles, CA 90089-0484, USA
[b] Mork Family Department of Chemical Engineering and Materials Science, University of Southern California, Los Angeles, CA 90089-1211, USA
[c] Core Center of Excellence for Nano Imaging (CNI), University of Southern California, Los Angeles, CA 90089-0101, USA
[d] Security and Disruptive Technologies, National Research Council Canada, Ottawa, Ontario K1A 0R6, Canada

ARTICLE INFO

Keywords:
Single-walled carbon nanotubes
Size-selected nanoparticles
Soft landing
Deposition

ABSTRACT

We describe a technique to prepare ensembles of neat, unbundled single-walled carbon nanotubes decorated with pure size-filtered metal nanoparticles. Polymer-encased nanotubes are drop-cast on nanoporous transmission electron microscope membrane grids, mounted within a nanoparticle-deposition apparatus, baked in situ to remove the polymer coating, and exposed to a beam of pure size-selected metal nanoparticles. Subsequent electron microscopy imaging reveals the presence of nanoparticles supported by pure suspended single-walled nanotubes. This method is promising for efficient production of prototype chemical and physical devices which require the presence of clean well-defined nanoparticle-nanotube hybrids for characterization, imaging, and applications.

1. Introduction

Carbon nanotubes decorated with metal nanoparticles have the potential to integrate the distinctive mechanical and electronic properties of nanotubes with the size- and material-dependent tunability of metal particle characteristics. These quintessentially nanoscale hybrids have been explored for applications in catalysis and fuel cell research (see, e.g., [1–3] and the reviews [4–6]), gas sensing [7–11], and photovoltaics [12].

Nanoparticle integration with carbon nanotubes ("CNTs") has been performed by both "chemical adhesion" and "physical deposition" methods. The former approach employs surface functionalization, precipitation, colloidal wetting, and electrolysis (see, e.g., [1,13–15] and the reviews [4,16]). The latter approach, in turn, involves gas-phase deposition of atomic vapor or preformed nanoparticles onto CNT surfaces by making use of thermal or electron-beam evaporation [7,17,18], magnetron sputtering [2,3,6,8,11,19,20], arc discharge [21,22], or laser ablation [23].

There are a number of aspects to these investigations which motivate further work. First of all, in most of them the exact nanoparticle size and morphology are neither controlled or preselected, nor precisely known. This requires the particles to be preformed, size-filtered, and soft-landed (see, e.g., [23]). Secondly, chemical methods introduce defects, impurities, and/or ligands, all of which are detrimental to device applications. And thirdly. the CNT substrates are typically multi-walled, as well as frequently highly bundled. (Single-walled CNTs were used in [7,17,18], but the nanoparticles were formed by diffusion and coagulation of adatoms, i.e., not in a size selective manner.)

It is desirable to develop samples where all of these facets are controlled: the CNTs are single-walled (SWCNTs) and ligand-free, and the metal nanoparticles are pure, size-selected, and soft-landed. This is of value for understanding nanoparticle-tube interactions in detail, for optimizing the performance of sensors, catalysts, etc. at the microscopic level, for improved imaging and diffraction capabilities, and for synthesizing nanowires and tunneling networks out of nanoparticle-coated CNTs.

Furthermore, in investigating well-defined SWCNT-nanoparticle contacts, it is also highly desirable to reduce bundling, to which nanotubes are highly prone in a liquid medium. This is a serious drawback, for example, in working with commercial CNT powder or "paper." One option is to grow the nanotubes directly on catalyst-coated microgrids by chemical vapor deposition [17,18], but this is a low-yield process in terms of the coverage density.

Here we describe an efficient and scalable approach to SWCNT-nanoparticle integration. A dispersion of preformed polymer-wrapped SWCNTs is prepared, deposited on TEM grids, heat treated to remove

* Corresponding author.
E-mail address: kresin@usc.edu (V.V. Kresin).

https://doi.org/10.1016/j.tsf.2020.137907
Received 20 December 2019; Received in revised form 11 February 2020; Accepted 28 February 2020
Available online 29 February 2020

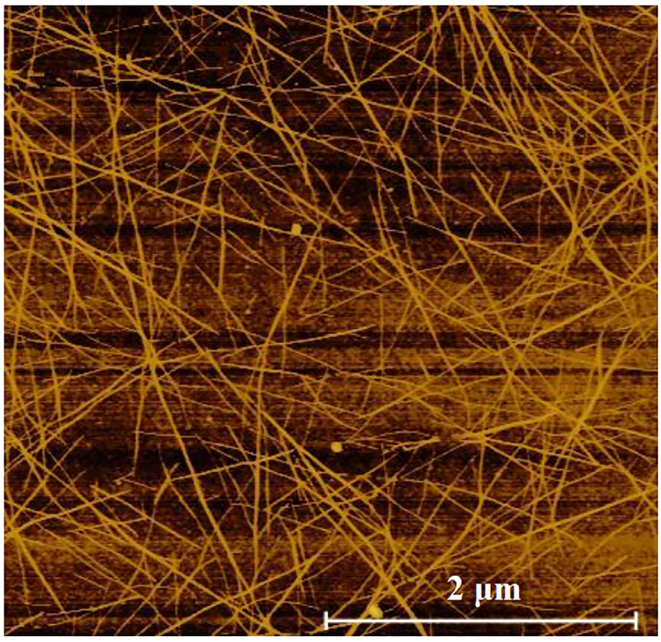

Fig. 1. An AFM image of polymer-coated single-wall carbon nanotubes on a SiO_2 surface, illustrating the absence of substantial bundling in the suspension mixture.

the polymer coating, and exposed to a beam of pure size-selected metal nanoparticles. Imaging by transmission electron microscopy (TEM) confirms the presence of supported nanoparticles and nanoparticle chains on SWCNT side walls. Thus, without any post-treatment this technique yields an ensemble of archetypal nanotube-nanoparticle junctions: intact size-selected metal nanoparticles supported by intact suspended SWCNTs.

2. Sample preparation

The base material for the process is a dried film of semiconducting SWCNTs. The nanotubes were fabricated in an electric arc discharge reactor and high purity semiconducting SWCNTs with a distribution of chiralities were isolated using conjugated polymer extraction [24–27]. The polymer coating, characterized as "non-covalent exohedral functionalization" [28], is the ingredient responsible both for preventing severe bundling when the nanotube powder is dispersed into a liquid suspension and for preventing chemical and physical damage to the nanotube walls during deposition on a grid substrate.

After much trial and error, the following protocol was found to result in a suitable density of nanotube deposition. A 0.12 mg/ml homogeneous suspension was prepared by adding 1.2 mg of the dry film to 10 ml of anhydrous toluene and sonicating it in an ultrasonic bath for 30 min. Atomic force microscopy (AFM) imaging of this dispersion drop-casted on a SiO_2 substrate was used to confirm the essentially unbundled nature of the resulting coverage and to fine-tune

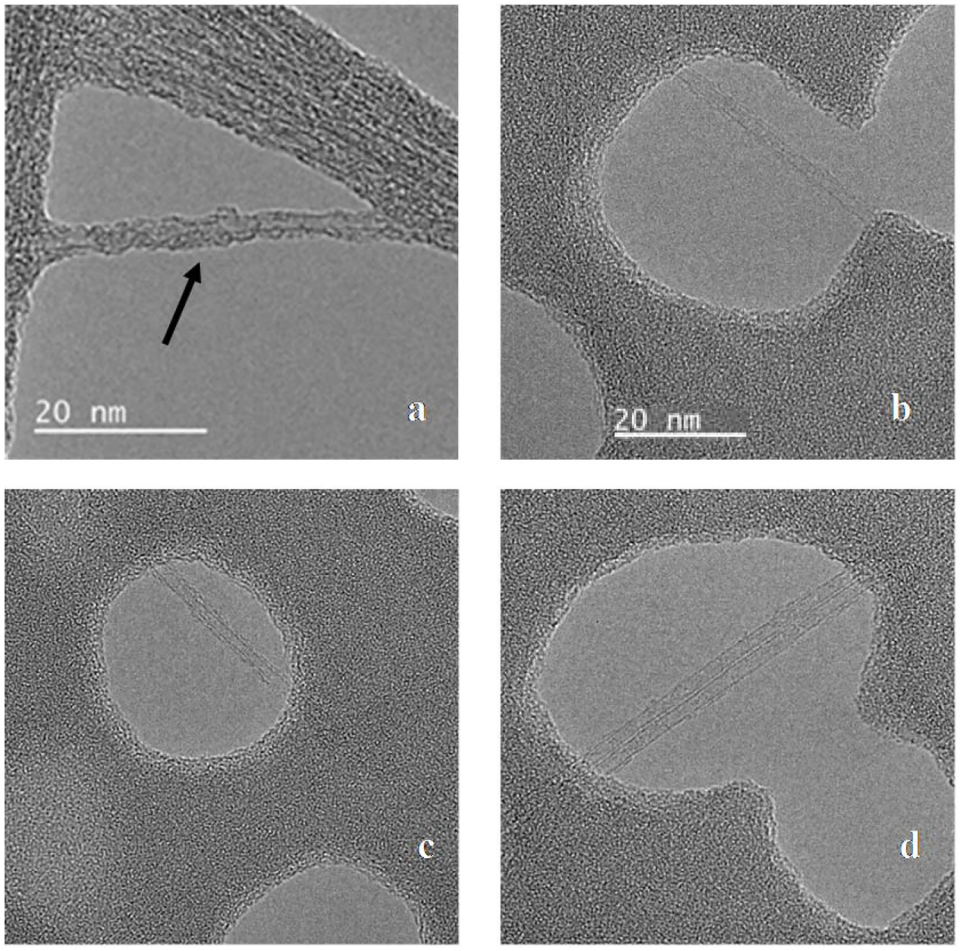

Fig. 2. (a) TEM image of a suspended SWCNT without heat treatment, showing (arrow) the carbonaceous layer developed from electron beam impact on the nanotube's polymer coating.(b,c) TEM images of individual SWCNTs bridging pores of SiN TEM grids after vacuum bakeout. The average nanotube diameter is 1.5 nm. Image (d) shows twin suspended SWCNTs with a clean gap between them, confirming that the bakeout leaves no trace of polymer on the nanotubes.) Panels (b–d) have the same scale.

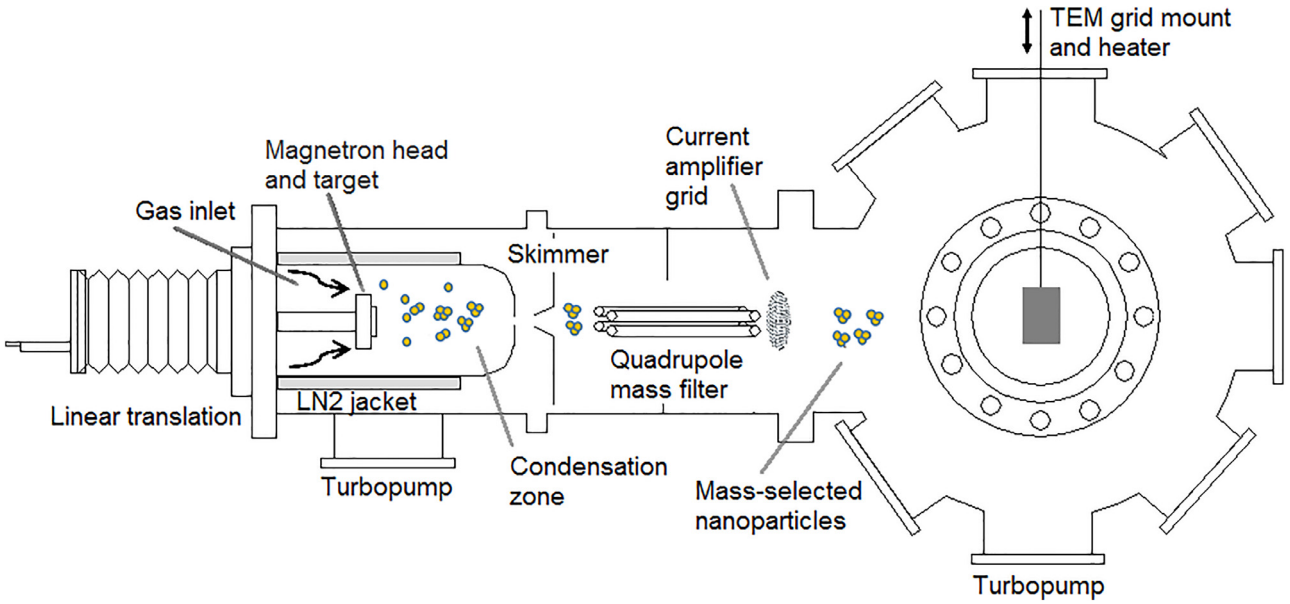

Fig. 3. Outline of the nanoparticle deposition apparatus. Metal atoms are generated by magnetron sputtering and enter the liquid-nitrogen-cooled condensation zone, where they undergo collisions with cold argon and helium gases. Nanoparticle ions nucleate and grow as the vapor moves through the source toward the source exit aperture. The ions are filtered by a quadrupole mass analyzer equipped with an ion flux measurement grid and enter the deposition chamber. Here they are deposited directly onto single-walled carbon nanotubes suspended on nanoporous silicon nitride TEM grids. The grid support also houses a heater used for in situ removal of the nanotubes' polymer coating prior to nanoparticle deposition.

the amount required for covering TEM grids, see Fig. 1. Consistent with this figure, subsequent electron microscopy images (see below) showed that bridges over the TEM grid pores were composed of single nanotubes, or at most just thin strands of a few parallel nanotubes. A lower concentration of nanotube suspension yields too few pore-bridging nanotubes after the spin-coating described below. At higher concentrations the CNTs are still effectively protected from bundling by the polymer wrapping, but increasingly overlap into a network that covers up the pore openings.

The grids are "nanoporous" amorphous silicon nitride films, 20 nm thick with an average pore opening of 30 nm (TEMwindows.com, product code SN100-P20Q05). Despite being mechanically very delicate, they offer a convenient combination of porosity and TEM contrast for imaging CNT samples. These grids also are uniquely suitable for high-temperature nanotube bakeout that is described below. (They are also available with 2 μm pore sizes, which could provide a greater open area but is a challenging dimension to bridge with the nanotubes; this is to be investigated in future work.)

A 10 μl pipette was used to cast a drop of SWCNT solution on the grids, which were then spun in a spin coater for 10 s at 50 rpm and 60 s at 100 rpm. This spinning sequence was then repeated. This coating procedure promptly removes excess moisture from the fragile TEM grid membrane while avoiding mechanical damage to the latter, and provides a degree of alignment to the nanotubes settling onto the grid.

As illustrated by Fig. 2(a), at this stage the SWCNTs' wrapping polymer must be removed. This was done by mounting the TEM grids on a homebuilt heating stage positioned directly within the nanoparticle deposition chamber and carefully baking them at 400 °C for 10 h under high vacuum (5×10^{-7} Pa base pressure). As is demonstrated in Figs. 2(b–d), this yielded pristine nanotubes with diameters in the range of 1–2 nm, with many of them spanning the nanoscale pores of the TEM grids.

In order to keep the SWCNT coated grids free from post-contamination, nanoparticle beam deposition took place as soon as the samples cooled down from the bakeout procedure. In this work we deposited aluminum and copper nanoparticles as test systems.

Nanoparticles were produced by a Mantis Deposition Nanogen-50 source shown in Fig. 3. It operates by magnetron sputtering of atoms from a metal target followed by their condensation within a flowing cold inert gas [29,30]. The magnetron block was equipped with the manufacturer's "magnet set A" which produces primarily ionized particles (of which over 80% are anions, per manufacturer documentation, see also [31]). Argon and helium gases were introduced at controlled flow rates into the sputtering and nucleation regions, and the length of the condensation path could be varied by translating the magnetron head toward or away from the source exit aperture. All of these parameters affect the intensity and size distribution of nanoparticle production; the interplay between them has been discussed in detail, e.g., in [32].

After leaving the source, the nanoparticle ions passed through a high-range quadrupole mass filter (Mantis MesoQ) with a nominal mass range of ~300–10^6 u and landed on the CNT-supporting TEM grids described above. In the present set of experiments, the mass filter transmitted particles with average diameter of 7 nm and a size resolution of ~20%. TEM images presented below are consistent with this setting. The resolution and size were selected for high deposition current and easier TEM imaging, respectively, however the arrangement is capable of depositing larger or smaller nanoparticles, and a tighter size selectivity, when desired.

At this point the grid support block was held at room temperature and was grounded, neutralizing the deposited ions. The incoming ion current was measured by a Keithley 6487 picoammeter to be typically in the range of ~0.1 nA. Since the beam atom was below ~0.1 eV, lying below the atomic binding energy, this is considered to correspond to the "soft-landing" regime which avoids significant fragmentation and deformation of the nanoparticles and nanotubes [33]. This was confirmed by TEM images described below.

3. Imaging

For imaging, the samples were removed from the deposition system and transferred to a JEOL JEM-2100F TEM. To reduce knock-on damage and sputtering, the high tension of the transmission electron microscope was set to 80 kV.

Sample images produced after aluminum nanoparticle deposition are shown in Fig. 4. Fig. 4(a) includes a chain of nanoparticles aligned

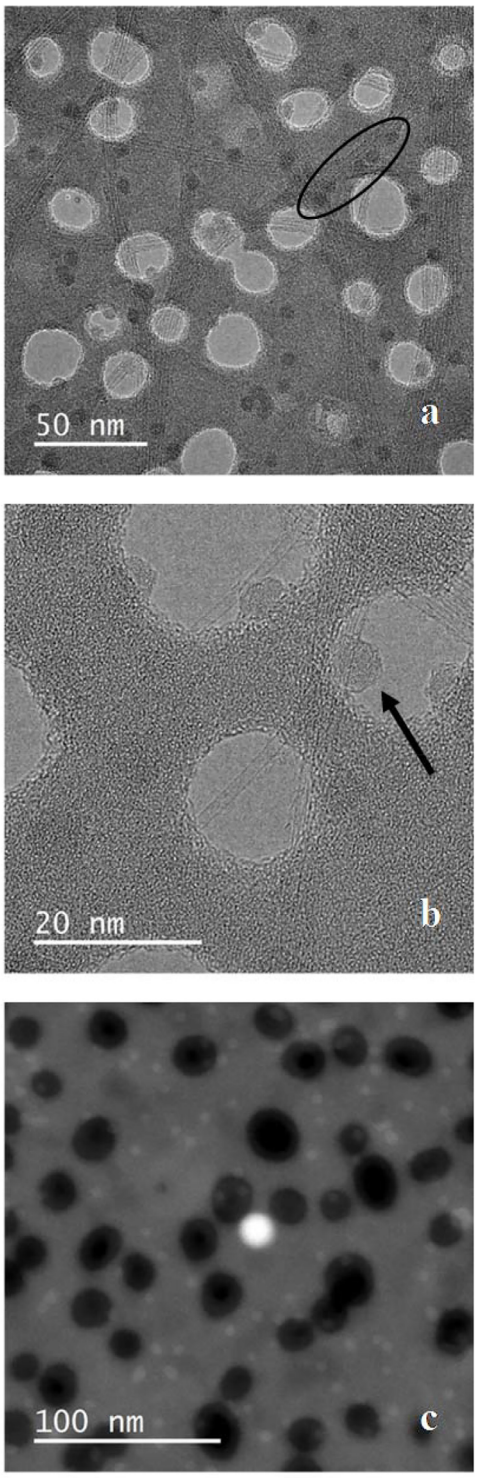

Fig. 4. TEM images of Al nanoparticles landed on SWCNTs on a nanoporous SiN TEM grid. (a) The oval highlights a chain of nanoparticles aligned along the nanotube sidewall. (b) A deposited aluminum nanocluster (arrow) on a suspended SWCNT. (c) A lower-magnification annular dark field scanning TEM image shows nanoparticles (gray) suspended over the grid's nanopores (dark). (The bright spot is an artifact due to the electron beam.) Nanoparticle coverage at the level shown in these images was obtained within 8 min of deposition time.

along a nanotube on the grid membrane, while Fig. 4(b) and (c) illustrate nanoparticles supported by individual SWCNTs over the membrane openings. The bare parts of the nanotubes themselves remain damage- and contamination-free. Fig. 5(a) shows an image where individual nanoparticles are supported by strands of three parallel nanotubes. Fig. 5(b) shows an analogous example of preselected copper nanoparticles supported by pristine SWCNTs over a TEM grid nanopore.

Since the samples were transported in air, it is expected that the imaged nanoparticles are mostly oxidized. (Aluminum nanoparticles are believed to develop an oxide layer to a thickness of ~3–4 nm [34]; indeed, our TEM images revealed predominantly amorphous oxide nanoparticle structures.) Their positions however represent the original placement, which is of main interest in the present report. Depending on the application, oxidation can be avoided by the use of unreactive materials such as gold, or by in situ processes. Alternatively, nanoscale oxides coated on SWCNTs could be exploited for catalysis and sensing.

4. Conclusions

In summary, we have demonstrated a straightforward and powerful method of obtaining high-yield, high-purity nanoparticle-nanotube hybrids. Abundant surface coverage of uncontaminated, highly debundled single-walled carbon nanotubes was achieved by drop-casting a dispersion of polymer-wrapped SWCNTs followed by careful heat treatment to remove the polymeric excipient. To create an ensemble of suspended nanotubes, they were deposited on nanoporous silicon nitride membranes. After polymer removal, the nanotubes were then decorated with ligand- and impurity-free metal nanoparticles by exposing them to a beam of nanoparticle ions which were prepared in a magnetron sputtering/vapor condensation source and size selected by a high-range quadrupole mass filter. Electron microscopy images confirmed the presence of nanoparticles supported by nanotubes suspended over nanoscale pores, and/or aligned along the nanotube walls. Compared to other physical and chemical methods, this technique enables efficient production of decorated nanotubes while maintaining control over the size, composition, coverage, and morphology of the supported nanoparticles.

Pristine suspended nanoparticle-nanotube systems of this type can be utilized for high-resolution imaging of the atomic structure of nanoparticles, as no membrane is present in the path of the electron beam. They are also promising for the study of size-dependent particle-tube wall interactions and as novel catalytic systems. For instance, recent work [35] demonstrated the effectiveness of molecular catalysts immobilized on the surface of carbon nanotubes. An analogous system of size-selected catalytically active nanoparticles on SWCNT surfaces is therefore of definite interest and, as demonstrated here, can be synthesized in an efficient manner.

Further applications can include the alignment of metal nanoparticles along SWCNTs for the formation of tunneling nanoparticle arrays for chemical sensing (cf. [36]), plasmonic optical chains (cf. [37], and high-performance superconducting electronics networks utilizing high-temperature superconducting nanoclusters (cf. [38,39]).

The nanotube and nanoparticle coverage densities in this work were specifically optimized toward the goal of obtaining hybrids of individual, resolvable particles with individual single-walled carbon nanotubes. For applications where higher densities are desired and suitable, the same described technique can be applied to generate concentrated SWCNT networks covered with full monolayers (or multilayers) of size-selected nanoparticles.

CRediT authorship contribution statement

Malak Khojasteh: Methodology, Investigation, Validation, Writing - review & editing. **Matthew H. Mecklenburg:** Methodology, Investigation, Resources, Writing - review & editing. **Patrick J. Edwards:** Validation, Writing - review & editing. **Jacques Lefebvre:** Resources. **Jianfu Ding:** Resources. **Patrick R.L. Malenfant:** Resources, Writing - review & editing. **Vitaly V. Kresin:** Conceptualization, Supervision, Writing - review & editing, Funding

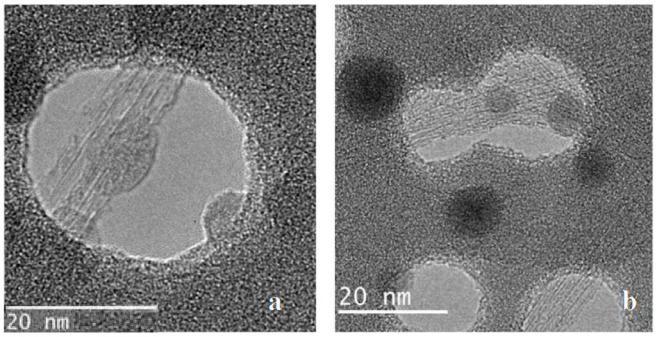

Fig. 5. (a) TEM image of an Al nanoparticle landed on three parallel SWCNTs suspended over openings in a nanoporous SiN TEM grid. (b) TEM image of individual Cu nanoparticles supported by SWCNTs over a nanopore.

acquisition.

Declaration of Competing Interest

The authors declare that they have no known competing financial interests or personal relationships that could have appeared to influence the work reported in this paper.

Acknowledgments

The images shown in this article were acquired at the USC Core Center of Excellence in Nano Imaging (CNI). This work was supported by the Army Research Office under Grant number W911NF-17-1-0154 and by the U.S. National Science Foundation under grant CHE-1664601.

References

[1] J.M. Planeix, N. Coustel, B. Coq, V. Brotons, P.S. Kumbhar, R. Dutartre, P. Geneste, P. Bernier, P.M. Ajayan, Application of carbon nanotubes as supports in heterogeneous catalysis, J. Am. Chem. Soc. 116 (1994) 7935–7936.
[2] K. Yoshii, K. Yamaji, T. Tsuda, H. Matsumoto, T. Sato, R. Izumi, T. Torimoto, S. Kuwabata, Highly durable Pt nanoparticle-supported carbon catalysts for the oxygen reduction reaction tailored by using an ionic liquid thin layer, J. Mater. Chem. A. 4 (2016) 12152–12157.
[3] S. Hussain, H. Erikson, N. Kongi, M. Merisalu, P. Ritslaid, V. Sammelselg, K. Tammeveski, Heat-treatment effects on the ORR activity of Pt nanoparticles deposited on multi-walled carbon nanotubes using magnetron sputtering technique, Int. J. Hydrog. Energ. 42 (2017) 5958–5970.
[4] G.G. Wildgoose, C.E. Banks, R.G. Compton, Metal nanoparticles and related materials supported on carbon nanotubes: methods and applications, Small 2 (2006) 182–193.
[5] P. Serp, E. Castillejos, Catalysis in carbon nanotubes, ChemCatChem 2 (2010) 41–44.
[6] O.K. Alexeeva, V.N. Fateev, Application of the magnetron sputtering for nanostructured electrocatalysts synthesis, Int. J. Hydrog. Energ. 41 (2016) 3373–3386.
[7] J. Kong, M.G. Chapline, H. Dai, Functionalized carbon nanotubes for molecular hydrogen sensors, Adv. Mater. 13 (2001) 1384–1386.
[8] Y. Lu, J. Li, J. Han, H.T. Ng, C. Binderik, C. Partridge, M. Meyyappan, Room temperature methane detection using palladium loaded single-walled carbon nanotube sensors, Chem. Phys. Lett. 391 (2004) 344–348.
[9] M. Penza, R. Rossi, M. Alvisi, M.A. Signore, G. Cassano, D. Dimaio, R. Pentassuglia, E. Piscopiello, E. Serra, M. Falconieri, Characterization of metal-modified and vertically-aligned carbon nanotube films for functionally enhanced gas sensor applications, Thin Solid Films 517 (2009) 6211–6216.
[10] D.R. Kauffman, D.C. Sorescu, D.P. Schofield, B.L. Allen, K.D. Jordan, A. Star, Understanding the sensor response of metal-decorated carbon nanotubes, Nano Lett. 10 (2010) 958–963.
[11] P.R. Mudimela, M. Scardamaglia, O. González-León, N. Reckinger, R. Snyders, E. Llobet, C. Bittencourt, J.-F. Colomer, Gas sensing with gold-decorated vertically aligned carbon nanotubes, Beilstein J. Nanotechnol. 5 (2014) 910–918.
[12] P.R. Somani, S.P. Somani, M. Umeno, Application of metal nanoparticles decorated carbon nanotubes in photovoltaics, Appl. Phys. Lett. 93 (2008) 033315.
[13] R. Voggu, S. Pal, S.K. Pati, C.N.R. Rao, Semiconductor to metal transition in SWNTs caused by interaction with gold and platinum nanoparticles, J. Phys. 20 (2008) 215211.
[14] M. Barberio, F. Stranges, F. Xu, Coating geometry of Ag, Ti, Co, Ni, and Al nanoparticles on carbon nanotubes, Appl. Surf. Sci. 334 (2015) 174–179.
[15] Z.P. Michael, W. Shao, D.C. Sorescu, R.W. Euler, S.C. Burkert, A. Star, Probing biomolecular interactions with gold nanoparticle-decorated single-walled carbon nanotubes, J. Phys. Chem. C 121 (2017) 20813–20820.
[16] V. Georgakilas, D. Gournis, V. Tzitzios, L. Pasquato, D.M. Guldie, M. Prato, Decorating carbon nanotubes with metal or semiconductor nanoparticles, J. Mater. Chem. 17 (2007) 2679–2694.
[17] Y. Zhang, H. Dai, Formation of metal nanowires on suspended single-walled carbon nanotubes, Appl. Phys. Lett. 77 (2000) 3015–3017.
[18] Y. Zhang, N.W. Franklin, R.J. Chen, H. Dai, Metal coating on suspended carbon nanotubes and its implication to metal–tube interaction, Chem. Phys. Lett. 331 (2000) 35–41.
[19] M. Scarselli, L. Camilli, P. Castrucci, F. Nanni, S. Del Gobbo, E. Gautron, S. Lefrant, M. De Crescenzi, In situ formation of noble metal nanoparticles on multiwalled carbon nanotubes and its implication in metal–nanotube interactions, Carbon N Y 50 (2012) 875–884.
[20] C. Muratore, A.N. Reed, J.E. Bultman, S. Ganguli, B.A. Cola, A.A. Voevodin, Nanoparticle decoration of carbon nanotubes by sputtering, Carbon N Y 57 (2013) 274–281.
[21] L. Zhu, G. Lu, S. Mao, J. Chen, D.A. Dikin, X. Chen, R.S. Ruoff, Ripening of silver nanoparticles on carbon nanotubes, Nano 2 (2007) 149–156.
[22] J. Chen, G. Lu, Controlled decoration of carbon nanotubes with nanoparticles, Nanotechnology 17 (2006) 2891–2894.
[23] L. Bardotti, F. Tournus, R. Delagrange, J.-M. Benoit, O. Pierre-Louis, V. Dupuis, Behavior of size selected iron–platinum clusters soft landed on carbon nanotubes, Appl. Surf. Sci. 301 (2014) 564–567.
[24] J. Ding, Z. Li, J. Lefebvre, F. Cheng, J.L. Dunford, P.R.L. Malenfant, J. Humes, J. Kroeger, A hybrid enrichment process combining conjugated polymer extraction and silica gel adsorption for high purity semiconducting single-walled carbon nanotubes (SWCNT), Nanoscale 7 (2015) 15741–15747.
[25] Z. Li, J. Ding, J. Lefebvre, P.R.L. Malenfant, Surface effects on network formation of conjugated polymer wrapped semiconducting single walled carbon nanotubes and thin film transistor performance, Org. Electron 26 (2015) 15–19.
[26] J. Lefebvre, J. Ding, Z. Li, P. Finnie, G. Lopinski, P.R.L. Malenfant, High-purity semiconducting single-walled carbon nanotubes: a key enabling material in emerging electronics, Acc. Chem. Res. 50 (2017) 2479–2486.
[27] Z. Li, J. Ding, J. Lefebvre, P.R.L. Malenfant, Dopant-modulated conjugated polymer enrichment of semiconducting SWCNTs, ACS Omega 3 (2018) 3413–3419.
[28] A. Hirsch, Functionalization of single-walled carbon nanotubes, Angew. Chem. Int. Ed. 41 (2002) 1853–1859.
[29] H. Haberland, U. Buck, G. Scoles, Experimental methods, in: H. Haberland (Ed.), Clusters of Atoms and Molecules: Theory, Experiment, and Clusters of Atoms, Springer, Berlin, 1994, pp. 207–252.
[30] Y. Huttel (Ed.), Gas-Phase Synthesis of Nanoparticles, Wiley-VCH, Weinheim, 2017.
[31] M. Khojasteh, Fabrication, deposition, and Characterization of Size-Selected Metal Nanoclusters With a Magnetron Sputtering Gas Aggregation Source, University of Southern California, Los Angeles, 2019 Ph.D. dissertation.
[32] M. Khojasteh, V.V. Kresin, Influence of source parameters on the growth of metal nanoparticles by sputter-gas-aggregation, Appl. Nanosci. 7 (2017) 875–883.
[33] V.N. Popok, I. Barke, E.E.B. Campbell, K.-H. Meiwes-Broer, Cluster-surface interaction: from soft landing to implantation, Surf. Sci. Rep. 66 (2011) 347–377.
[34] A. Perron, S. Garruchet, O. Politano, G. Aral, V. Vignal, Oxidation of nanocrystalline aluminum by variable charge molecular dynamics, J. Phys. Chem. Solids 71 (2010) 119–124.
[35] Y. Wu, Z. Jiang, X. Lu, Y. Liang, H. Wang, Domino electroreduction of CO_2 to methanol on a molecular catalyst, Nature 575 (2019) 639–642.
[36] J. van Lith, A. Lassesson, S.A. Brown, M. Schulze, J.G. Partridge, A. Ayesh, A hydrogen sensor based on tunneling between palladium clusters, Appl. Phys. Lett. 91 (2007) 181910.
[37] V.V. Kravets, L.E. Ocola, Y. Khalavka, A.O. Pinchuk, Polarization and distance dependent coupling in linear chains of gold nanoparticles, Appl. Phys. Lett. 106 (2015) 053104.
[38] Y.N. Ovchinnikov, V.Z. Kresin, Cluster-based superconducting tunneling networks, Phys. Rev. B 85 (2012) 064518.
[39] A. Halder, V.V. Kresin, Spectroscopy of metal 'superatom' nanoclusters and high-T_c superconducting pairing, Phys. Rev. B 92 (2015) 214506.